

Majorana-time-reversal symmetries: a fundamental principle for sign-problem-free quantum Monte Carlo simulations

Zi-Xiang Li, Yi-Fan Jiang, and Hong Yao*

Institute for Advanced Study, Tsinghua University, Beijing 100084, China

(Dated: December 3, 2024)

A fundamental open issue in physics is whether and how the fermion-sign-problem in quantum Monte Carlo (QMC) can be solved generically. Here, we show that Majorana-time-reversal (MTR) symmetries can provide a unifying principle to solve the fermion-sign-problem in interacting fermionic models. By systematically classifying Majorana-bilinear operators according to the anti-commuting MTR symmetries they respect, we rigorously proved that there are two and only two fundamental symmetry classes which are sign-problem-free and which we call “Majorana-class” and “Kramers-class”. All other sign-problem-free symmetry classes have higher symmetries than these two fundamental classes. Sign-problem-free models in the Majorana-class include interacting topological superconductors, for which we performed sign-problem-free Majorana QMC simulations and found that with increasing interactions the topological superconductor’s helical edge states first undergo spontaneous symmetry-breaking while the bulk is still topologically-nontrivial. Remarkably, we discovered emergent spacetime supersymmetry (SUSY) at the edge quantum critical point.

Interactions between particles are ubiquitous and studying interacting models of many-body systems is of central importance in modern condensed matter physics and other fields[1–3]. However, many interesting models in two and three dimensions, especially those with strong interactions, are beyond the solvability of any known analytical methods. Consequently, developing efficient and un-biased numerical methods plays a key role in understanding many-body physics in solid state materials like high temperature superconductors as well as in other systems such as quark matters. Because quantum Monte Carlo (QMC) is numerically-exact and intrinsically-unbiased, it is one of the most important numerical methods to study interacting many-body systems[4–6]. Unfortunately, QMC often encounters the notorious fermion-sign-problem, the presence of which makes it practically infeasible to study those models with large system sizes and at low temperature[7].

Even though a general solution of the fermion-sign-problem is nondeterministic polynomial (NP) hard[8], many specific interacting models have been successfully identified to be sign-problem-free. One prototype sign-problem-free example is the repulsive Hubbard model

# of anti-commuting MTR symmetries	Sign-problem-free	Sign-problem
0		$\{I\}$ = no symmetry
1		$\{T_1^+\}$ $\{T_1^-\}$
2	$\{T_1^+, T_2^-\}$ = Majorana-class $\{T_1^-, T_2^-\}$ = Kramers-class	$\{T_1^+, T_2^+\}$
3	$\{T_1^+, T_2^+, T_3^-\}$ $\{T_1^+, T_2^-, T_3^-\}$ $\{T_1^-, T_2^-, T_3^-\}$	$\{T_1^+, T_2^+, T_3^+\}$
≥ 4	all	

FIG. 1. The “periodic table” of sign-problem-free symmetry classes defined by the set of anti-commuting Majorana-time-reversal symmetries $\{T_1^{p_1}, T_2^{p_2}, \dots, T_n^{p_n}\}$ they respect, where $p_i = \pm$ and $(T_i^\pm)^2 = \pm 1$. We proved that there are two and only two *fundamental* symmetry classes which are sign-problem-free: Majorana-class and Kramers-class. For the former, Majorana-bilinear operators possess two anti-commuting MTR symmetries T_1^+ and T_2^- with $T_1^+T_2^- = -T_2^-T_1^+$. This symmetry class was originally proposed by three of us (LJY) in Ref. [12] where the Majorana representation for QMC was introduced for the first time. For the latter, there are two anti-commuting MTR symmetries T_1^- and T_2^- , from which conventional Kramers-symmetry can be derived.

at half-filling [4–6]. In the language of auxiliary-field QMC[4–6], the partition function $Z = \sum \rho$, where the Boltzmann weight $\rho = \text{Tr} \prod_{i=1}^{N_\tau} \exp[\hat{h}_i]$ with \hat{h}_i being fermion-bilinear operators depending on auxiliary-fields at imaginary time τ_i . If all Boltzmann weight $\rho > 0$, the simulation is free from the fermion-sign-problem and the needed computation time grows only polynomially with the system size and inverse temperature. It is desired to construct a fundamental principle for identifying interacting fermion models which are sign-problem-free.

One successful strategy of solving the sign-problem is to employ the Kramers-symmetry of fermion-bilinear operators \hat{h}_i , which is defined as having both time-reversal symmetry $\hat{\Theta}$ and charge-conservation \hat{Q} with $[\hat{\Theta}, \hat{Q}] = 0$ and $\hat{\Theta}^2 = -1$. With the Kramers-symmetry, eigenvalues always appear in Kramers pairs such that the Boltzmann weight can be shown to be positive-definite[9–11]. Sign-problem-free models with Kramers-symmetry have been studied extensively during the past three decades.

Quite recently, Majorana representation was first introduced by three of us (LJY) in Ref. [12] to solve the sign-problem in models which are beyond the Kramers method. We employed the time-reversal symmetry in

the Majorana representation to prove that a large class of interesting models can be free from the fermion-sign-problem. Remarkably, such sign-problem-free models introduced in Ref. [12] include interacting models of spinless, spinful, and even SU(3) fermions, many of which are beyond the applicability of the Kramers method discussed above. Novel phenomena such as fermion-induced quantum critical points (FIQCP) were discovered in such sign-problem-free models by large-scale QMC simulations[13].

In this work, we systematize the idea of Majorana-time-reversal symmetry proposed in Ref. [12] to derive a fundamental and unifying principle to solve the sign-problem. Namely, we classify Majorana-bilinear operators $\hat{h} = \gamma^T h \gamma$ according to their Majorana-time-reversal symmetries, where $h^T = -h$ is an anti-symmetric matrix and $\gamma^T = (\gamma_1, \dots, \gamma_{2N})$ are Majorana operators with $\{\gamma_i, \gamma_j\} = 2\delta_{ij}$, and then identify all symmetry classes which must be sign-problem-free. Note that “time-reversal” in this work generally represents “anti-unitary”. Because Majorana are real fermions, Majorana-time-reversal transformation can be represented by $T = UK$, where U are *real* orthogonal matrices and K represents complex conjugation with $T^2 = \pm 1$ for $UT = \pm U$. By systematically classifying Majorana-bilinear operators according to the maximal set of anti-commuting MTR symmetries they respect, we prove that there are two and only two fundamental symmetry classes of models which are sign-problem-free: Majorana-class and Kramers-class. Other sign-problem-free symmetry classes have higher symmetries than the two fundamental ones.

For the Majorana-class, the Majorana-bilinear operators possess two anti-commuting symmetries T_1^+ and T_2^- , where $(T_i^\pm)^2 = \pm 1$. Majorana-bilinear operators in this class can always be transformed into two decoupled parts which are time-reversal partners to each other such that it is sign-problem-free [12]. For the Kramers-class, from the anti-commuting T_1^- and T_2^- , the usual Kramers-time-reversal symmetry can be constructed so that they are sign-problem-free. Interesting sign-problem-free strongly-correlated models in the Kramers-class have been studied by QMC recently to investigate physics in high-temperatures superconductors around quantum critical points [11, 14–18].

It is worth to point out that sign-problem-free models in the Majorana-class include interacting topological superconductors with helical edge states [19–21]. Note that the fermion-sign-problem of these models are certainly beyond the capability of the split-orthogonal-group method which requires particle number conservation [22]; in contrast, the Majorana approach introduced by us [12] and further studied in the present work is general and can be applied to generic models no matter the particle number is conserved or not. We perform sign-problem-free Majorana QMC simulations of two

interacting topological p -wave superconductors (one consisting of spin-1/2 electrons while the other spinless fermions) and find that with increasing interactions the topological superconductor’s edge states first undergo spontaneous symmetry-breaking while their bulks still preserve the symmetry (bulk symmetry-breaking occurs at stronger interaction strength). The critical exponents at the edge quantum critical points (QCP) obtained by our QMC simulations are almost perfectly consistent with the exact results of a spacetime supersymmetric theory, which provides convincing evidences that the edge QCP in helical Majorana edge states of topological superconductors feature an emergent spacetime SUSY [23, 24]. To the best of our knowledge, this is the first numerically-exact and unbiased study of two-dimensional microscopic models to discover an emergent spacetime SUSY.

Majorana-time-reversal symmetry classes and the “periodic table” of the fermion-sign-problem
Time-reversal symmetry plays a key role in classifying random matrices as well as topological insulators/superconductors[25–28], and in solving the fermion-sign-problem in QMC [9–11]. The Kramers-symmetry [9] has been a successful guiding principle for the sign-problem-free QMC simulations. Nonetheless, it was shown that it is not the most general time-reversal symmetry one can utilize to solve fermion-sign-problem [12]. It is then desired to construct a more fundamental and generic symmetry principle to solve the fermion-sign-problem.

In Ref. [12], we proposed that time-reversal symmetry in Majorana representation can be used to solve fermion-sign-problem in a large class of spinless and spinful models. We introduced the Majorana representation for fermions to write fermion-bilinear operators: $\hat{h}(\tau_i) \equiv \hat{h}_i = \gamma^T h_i \gamma$, where $\gamma^T = (\gamma_1^1, \dots, \gamma_N^1, \gamma_1^2, \dots, \gamma_N^2)$ and h_i is a $2N \times 2N$ matrix given by

$$h_i = \begin{pmatrix} B_i & 0 \\ 0 & B_i^* \end{pmatrix}. \quad (1)$$

It was shown [12] that $\rho = \text{Tr} \prod_{i=1}^{N_\tau} \exp[\hat{h}_i]$ is positive definite because of the Majorana-time-reversal symmetry $T^+ = \tau^x K$, under which $\gamma_i^1 \rightarrow \gamma_i^2$, $\gamma_i^2 \rightarrow \gamma_i^1$, and $B_i \rightarrow B_i^*$. Here τ^α Pauli matrices act in the Majorana-space (1, 2). Because no coupling terms between γ^1 and γ^2 exist in any \hat{h}_i , tracing over the Hilbert space of γ^1 and γ^2 can be done separately such that $\rho = \rho_1 \rho_2 > 0$ as $\rho_2 = \rho_1^*$ required by the Majorana-time-reversal symmetry [12]. This Majorana-time-reversal symmetry principle was applied not only to spinless fermions but also to spinful and even SU(3) fermions [12, 13].

Note that h_i in Eq. (1) also respects another Majorana-time-reversal symmetry $T^- = i\tau^y K$, besides $T^+ = \tau^x K$. Moreover, $T^- T^+ = -T^+ T^-$. One naturally asks the

following question: can any Majorana-bilinear operator with anti-commuting T^+ and T^- symmetries be transformed into the form in Eq. (1) such that it is sign-problem-free? The answer is positive, as shown below. This further motivates us to ask another question: can anti-commuting Majorana-time-reversal symmetries provide a fundamental principle to classify Majorana-bilinear operators such that the most general sufficient conditions for sign-problem-free models can be constructed? Our answer is also positive, as we prove below.

As Majorana are real fermions, Majorana-time-reversal symmetry can always be represented by $T^\pm = U^\pm K$, where $(T^\pm)^2 = \pm 1$ and U^\pm is a real orthogonal matrix satisfying $(U^\pm)^* = U^\pm$ and $(U^\pm)^T = \pm U^\pm$. We propose to systematically classify Majorana-bilinear operators according to the maximal set of anti-commuting MTR symmetries $\mathcal{C} = \{T_1^{p_1}, \dots, T_n^{p_n}\}$ they respect, namely $[T_i^{p_i}, h] = 0$ and $T_i^{p_i} T_j^{p_j} + T_j^{p_j} T_i^{p_i} = p_i 2\delta_{ij}$, where $p_i = \pm$. Because of the sign choices of p_i , there are totally $n + 1$ distinct symmetry classes for each n . For $n = 0$, there is only one symmetry class $\{I\}$, which means no Majorana-time-reversal symmetry can be found for Majorana-bilinear operators while for $n = 1$ there are two symmetry classes: $\{T_1^+\}$ and $\{T_1^-\}$. For $n = 2$ we have three symmetry classes: $\{T_1^+, T_2^+\}$, $\{T_1^+, T_2^-\}$, and $\{T_1^-, T_2^-\}$. Here, we only concern the symmetries of h_i , namely we assume that h_i are random matrices besides respecting the specified set of anti-commuting MTR symmetries. This classification scheme using anti-commuting symmetries is, in spirit, similar to the one employed by Kitaev in using the Clifford algebra to classify random matrices and construct the periodic table of topological insulators and superconductors[27].

Obviously, if a symmetry class \mathcal{C} is sign-problem-free, any higher symmetry class \mathcal{C}' , defined as the one whose symmetries can generate all the symmetries in \mathcal{C} , must be sign-problem-free. For instance, because the symmetry class $\{T_1^+, T_2^+, T_3^+, T_4^+\}$ also respects this set of anti-commuting MTR symmetries $\{T_1^+, T_2^-\}$ with $T_2^- = T_2^+ T_3^+ T_4^+$, the former class must be sign-problem-free if the latter one is sign-problem-free. Consequently, it would be sufficient to derive all the fundamental symmetry classes which are sign-problem-free.

It was known that sign-problem can appear in the following three symmetry classes: $\{I\}$, $\{T_1^+\}$, and $\{T_1^-\}$, as examples of negative signs in these three symmetry classes have been constructed. Consequently, symmetry requirement itself for these symmetry classes is not sufficient to guarantee the absence of fermion-sign-problem. We then move to the symmetry classes with $n = 2$ anti-commuting symmetries: $\{T_1^+, T_2^+\}$, $\{T_1^+, T_2^-\}$, and $\{T_1^-, T_2^-\}$. The symmetries in the class $\{T_1^+, T_2^+\}$ cannot guarantee the sign-problem-free because examples of sign-problem in this classes can be constructed. How about the other two classes $\{T_1^+, T_2^-\}$ and $\{T_1^-, T_2^-\}$? It turns out these two are fundamental symmetry classes

which are sign-problem-free, as we shall prove below.

Theorem: If Majorana-bilinear operators \hat{h}_i respect MTR symmetries in one of the two symmetry classes $\{T_1^+, T_2^-\}$ and $\{T_1^-, T_2^-\}$, the Boltzmann weight $\rho = \text{Tr} \prod_{i=1}^{N_\tau} \exp[\hat{h}_i] > 0$. Moreover, these two are only fundamental symmetry classes which are sign-problem-free.

We shall prove the theorem below for the two symmetry classes separately. We call the former symmetry class as “Majorana-class” while the latter one as “Kramers-class” for reasons which will be clear later.

Majorana-class: From the anti-commuting T_1^+ and T_2^- symmetries, a unitary symmetry $P = T_1^+ T_2^-$ can be obtained, which can be utilized to block diagonalize h_i into the form in Eq. (1). For this class of models whose Majorana-bilinear operators can be transformed into the block-diagonal form in Eq. (1), it was proved in Ref. [12] that they are sign-problem-free. Because charge-conservation is not required for this symmetry class, we call it the “Majorana-class”.

Kramers-class: From T_1^- and T_2^- symmetries, we can construct a unitary symmetry $Q = T_1^- T_2^-$. Because Q is anti-symmetric, namely $Q^T = -Q$, one can construct a charge operator $\hat{Q} = i\gamma^T Q \gamma$ and $[\hat{Q}, \hat{h}_i] = 0$. It is clear that the combination of T_1^- and Q in this symmetry class is equivalent to the Kramers-symmetry since $[T_1^-, Q] = 0$ and $(T_1^-)^2 = -1$. The absence of fermion-sign-problem was obvious because of the Kramers pairs in eigenvalues as shown in Ref. [9]. Because of the Kramers-symmetry, we denote this symmetry class as “Kramers-class”.

For symmetry classes with $n \geq 3$, it turns out that all of them, except only one class $\{T_1^+, T_2^+, T_3^+\}$, can generate the symmetries in either the Majorana-class or the Kramers-class. For instance, the symmetry class $\{T_1^+, T_2^+, T_3^-\}$ has higher symmetry than $\{T_1^+, T_2^-\}$ and $\{T_1^-, T_2^-, T_3^+\}$ higher than both $\{T_1^+, T_2^-\}$ and $\{T_1^-, T_2^+\}$. The only remaining unclear class is $\{T_1^+, T_2^-, T_3^+\}$, which cannot generate $\{T_1^+, T_2^-\}$ or $\{T_1^-, T_2^+\}$. Since examples of Majorana-bilinear operators with sign-problem have been found, the symmetries in this class cannot guarantee sign-problem-free.

Combining the results above, we have shown that there are two and only two fundamental sign-problem-free symmetry classes: the Majorana-class and the Kramers-class. The “periodic table” of symmetry classes which must be sign-problem-free is shown in Fig. 1, which provides a fundamental principle to identify sign-problem-free interacting models. *Q.E.D.*

Interacting topological superconductors in the Majorana-class and emergent supersymmetry

As mentioned above, there is no requirement of charge-conversation for sign-problem-free models in the Majorana-class. Consequently, interesting sign-problem free models describing interacting superconductors may be identified in this class such that we can study inter-

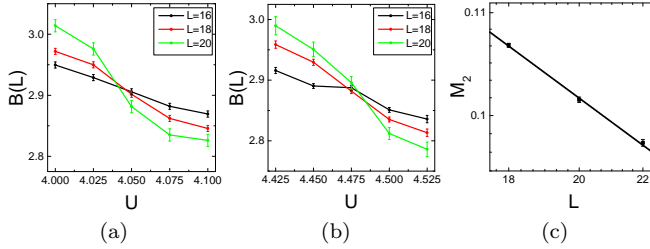


FIG. 2. Emergent SUSY at the edge QCP in the topological superconductor of spin-1/2 electrons studied by the sign-problem-free Majorana QMC. (a) From the Binder ratio on the edge, the edge QCP occurs $U_c^{\text{edge}} \approx 4.04$; (b) From the Binder ratio in the bulk, the bulk QCP happens at a stronger interaction strength $U_c^{\text{bulk}} \approx 4.575$; (c) From the log-log plot of the structure factor $M_2(L)$ versus L at the edge QCP $U = U_c^{\text{edge}}$, the anomalous dimension η fitted from the slope is $\eta = 0.43 \pm 0.04$, which is almost perfectly consistent with exact value of 0.40 predicted by the emergent SUSY.

action effect in superconductors using QMC. Indeed, we found two sign-problem-free models of interacting topological superconductors with helical edge states.

We first consider the Hamiltonian describing a topological superconductor of spin-1/2 electrons on the square lattice with time-reversal symmetry:

$$H = \sum_{ij,\sigma} [-t_{ij}c_{i\sigma}^\dagger c_{j\sigma} + \Delta_{ij,\sigma}c_{i\sigma}^\dagger c_{j\sigma}^\dagger + h.c.] - U \sum_i n_{i\uparrow} n_{i\downarrow}, \quad (2)$$

where $c_{i\sigma}^\dagger$ creates an spin-1/2 electron with $\sigma = \uparrow, \downarrow$, $n_{i\sigma} = c_{i\sigma}^\dagger c_{i\sigma}$, $t_{ij} = t$ is nearest-neighbor hopping, and $t_{ii} = \mu$ is the chemical potential. When $\Delta_{ij,\sigma} = \Delta$ for $j = i + \hat{x}$ and $\Delta_{ij,\sigma} = i\sigma\Delta$ for $j = i + \hat{y}$, the Hamiltonian in Eq. (2) describes a $(p + ip)_\uparrow(p - ip)_\downarrow$ -wave helical topological superconductor[27–29] with only triplet pairing, which hosts helical Majorana edge states protected by the usual time-reversal symmetry $T^- = i\sigma^y\tau^z K$, where σ^i acts in spin-space and τ^i in the Majorana-space. Besides T^- , it also possesses another time-reversal symmetry $T^+ = \sigma^x\tau^z K$ such that the topological classification of topological superconductors with both types of time-reversal symmetries is \mathbb{Z}_8 [19–21] instead of \mathbb{Z} or \mathbb{Z}_2 . For attractive Hubbard interactions, the fermion-bilinear operators obtained from the Hubbard-Stratonovich transform can also respect both T^+ and T^- such that this model is sign-problem-free in the Majorana-class, as shown in the Supplementary Materials (SM). Consequently, the interaction effect in such topological superconductors can be investigated by large-scale QMC simulations.

As the value of U/t is increased, the system is expected to encounter a quantum phase transition to a topologically-trivial superconductor with singlet pairing component, which spontaneously breaks the symmetry $P = T^-T^+ = \sigma^z\tau^0$. More remarkably, it was theoretically predicted that space-time supersymmetry should emerge at the quantum critical point of the helical Majorana edge states of the topological superconductors [23].

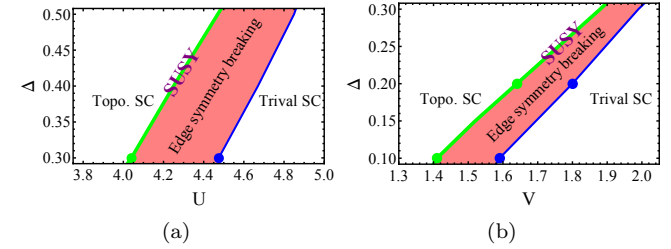


FIG. 3. Interacting topological superconductors with separated edge and bulk QCPs. There is an intermediate region where edge states have spontaneous symmetry breaking while the bulk is still disordered. The edge QCP features an emergent SUSY. The circles refer to data points. (a) The case of interacting topological superconductors of spin-1/2 electrons on the square lattice. (b) The case of interacting topological superconductors of spinless fermions on honeycomb lattice.

So far, numerically-exact and unbiased simulations of interacting topological superconductors and convincing evidences of emergent SUSY in a two-dimensional system are still lacking. We perform large-scale projector[30, 31], namely zero-temperature, QMC simulations of the sign-problem-free model in Eq. (2) to fill in the gap.

From computing the Binder ratio $B(L)$ of the order parameter $\langle c_{i\uparrow}^\dagger c_{i\downarrow}^\dagger \rangle$ on the square lattice with size $L \times L$ (see the SM for details), we first determine the critical values U_c^{edge} and U_c^{bulk} of spontaneous symmetry-breaking occurring on the edge and bulk, respectively, as shown in Fig. 2. The edge spontaneous symmetry breaking happens before the bulk does [32] such that there is a finite interaction range where the edge states are gapped out while the bulk still preserve the symmetry [see Fig. 3(a)]. At the edge QCP, emergent SUSY was predicted to occur from renormalization-group analysis and the exact value of anomalous dimension η is known to be $\eta_{\text{exact}} = 0.40$ according to the SUSY [33]. We computed η by QMC simulations at the edge QCP and obtained $\eta_{\text{QMC}} = 0.43 \pm 0.04$ which is almost perfectly consistent with exact value of 0.40 predicted by the emergent SUSY, which provides convincing evidence that the $\mathcal{N} = 1$ SUSY emerges at the edge QCP of the topological superconductors.

We further study an interacting topological superconductor of spinless fermions on honeycomb lattice which hosts helical Majorana edge states:

$$H = \sum_{\langle ij \rangle} (-t c_i^\dagger c_j + h.c.) + \sum_{\langle\langle ij \rangle\rangle} (\Delta c_i^\dagger c_j^\dagger + h.c.) + V \sum_{\langle ij \rangle} n_i n_j, \quad (3)$$

where c_i^\dagger creates a spinless fermion and $n_i = c_i^\dagger c_i$. When $\Delta = 0$, the sign-problem in this model can be solved in many ways [12, 22, 35]. However, when $\Delta \neq 0$, the fermion-sign-problem can only be solved by the Majorana method [12]. This model with $\Delta \neq 0$ is in the Majorana-class according to the classification in

the present work. Since it is sign-problem-free in the Majorana algorithm, we performed projector Majorana QMC of this interacting topological superconductor and also found strong evidence of emergent $\mathcal{N} = 1$ SUSY at the edge QCP: $\eta_{\text{QMC}} = 0.41 \pm 0.01$ is nearly the same as the exact value $\eta_{\text{exact}} = 0.40$, similar to the case of emergent SUSY at the edge QCP of the $(p+ip)\uparrow(p-ip)\downarrow$ -wave helical topological superconductor (see the SM for details).

Discussions and concluding remarks

We have shown that anti-commuting MTR symmetries can provide a fundamental principle to identify sign-problem-free interacting models. Assuming no other requirement than respecting a set of anti-commuting MTR symmetries, we have proved that there are two and only two fundamental sign-problem-free symmetry classes.

If the matrices h_i are not fully random besides respecting the required symmetries, it is possible that sign-problem-free models can be found in the symmetry classes $\{I\}$, $\{T_1^+\}$, $\{T_1^-\}$, $\{T_1^+, T_2^+\}$, and $\{T_1^+, T_2^+, T_3^+\}$ [34]. For instance, adding a staggered chemical potential $H_{\mu_s} = -\mu_s \sum_r (-1)^r c_r^\dagger c_r$ into Eq. (3) shall reduce its symmetries from the Majorana-class $\{T_1^+, T_2^-\}$ to $\{T_1^+\}$. It was shown in Ref. [35] that the model with H_{μ_s} is still sign-problem-free. This is because certain special condition is imposed on the matrix h_i by a staggered chemical potential. If adding a uniform chemical potential into Eq. (3), the sign-problem shall appear even though the symmetry classes for the staggered and uniform chemical potential are the same. In other words, it is still hopeful to solve the fermion-sign-problem in various interesting models, such as the repulsive Hubbard model away from half-filling [31], by utilizing special features not related to Majorana-time-reversal symmetries.

Acknowledgement.— We would like to thank Shao-Kai Jian and A. Kitaev for helpful discussions and the Milky Way II Supercomputer Center in Guangzhou for computational support. This work was supported by the National Thousand-Young-Talents Program (HY) and the NSFC under Grant No. 11474175 (ZXL, YFJ, and HY).

Note added.— While we were finishing the present manuscript, a related work appeared[36]. Our results are qualitatively similar when they overlap.

- [4] R. Blankenbecler, D. J. Scalapino, and R. L. Sugar, Phys. Rev. D **24**, 2278 (1981).
- [5] J. E. Hirsch, D. J. Scalapino, R. L. Sugar, and R. Blankenbecler, Phys. Rev. Lett. **47**, 1628 (1981).
- [6] J. E. Hirsch, Phys. Rev. B **31**, 4403 (1985).
- [7] E. Y. Loh, J. E. Gubernatis, R. T. Scalettar, S. R. White, D. J. Scalapino, and R. L. Sugar, Phys. Rev. B **41**, 9301 (1990).
- [8] M. Troyer and U.-J. Wiese, Phys. Rev. Lett. **94**, 170201 (2005).
- [9] C. Wu and S.-C. Zhang, Phys. Rev. B, **71**, 155115 (2005).
- [10] F. F. Assaad and H. G. Evertz, *Computational Many Particle Physics, Lecture Notes in Physics* **739**, 277 (2008).
- [11] E. Berg, M. A. Metlitski, and S. Sachdev, Science **338**, 1606 (2012).
- [12] Z.-X. Li, Y.-F. Jiang and H. Yao, Phys. Rev. B **91**, 241117 (2015).
- [13] Z.-X. Li, Y.-F. Jiang, S.-K. Jian, and H. Yao, arXiv:1512.07908 (2015).
- [14] Y. Schattner, S. Lederer, S. A. Kivelson, and E. Berg, arXiv:1511.03282 (2015).
- [15] Z.-X. Li, F. Wang, H. Yao, and D.-H. Lee, arXiv:1512.04541 (2015).
- [16] Z.-X. Li, F. Wang, H. Yao, and D.-H. Lee, arXiv:1512.06179 (2015).
- [17] Y. Schattner, M. H. Gerlach, S. Trebst, and E. Berg, arXiv:1512.07257 (2015).
- [18] P. T. Dumitrescu, M. Serbyn, R. T. Scalettar, and A. Vishwanath, arXiv:1512.08523 (2015).
- [19] X.-L. Qi, New J. Phys. **15**, 065002 (2013).
- [20] H. Yao and S. Ryu, Phys. Rev. B **88**, 064507 (2013).
- [21] S. Ryu and S.-C. Zhang, Phys. Rev. B **85**, 245132 (2012).
- [22] L. Wang, Y. H. Liu, M. Iazzi, M. Troyer and G. Harcos, Phys. Rev. Lett. **115**, 250601 (2015).
- [23] T. Grover, D. N. Sheng, A. Vishwanath, Science **344**, 280 (2014).
- [24] S.-K. Jian, Y.-F. Jiang, and H. Yao, Phys. Rev. Lett. **114**, 237001 (2015).
- [25] X.-L. Qi and S.-C. Zhang, Rev. Mod. Phys. **83**, 1057 (2011).
- [26] M. Z. Hasan and C. L. Kane, Rev. Mod. Phys. **82**, 3045 (2010).
- [27] A. Kitaev, in *Periodic Table for Topological Insulators and Superconductors* (AIP, New York, 2009) [AIP Conf. Proc. 1134, 22 (2009)].
- [28] A. P. Schnyder, S. Ryu, A. Furusaki, and A. W. W. Ludwig, Phys. Rev. B **78**, 195125 (2008).
- [29] X.-L. Qi, T. L. Hughes, S. Raghu, and S.-C. Zhang, Phys. Rev. Lett. **102**, 187001 (2009).
- [30] G. Sugiyama and S. Koogin, Annals of Phys. **168**, 1 (1986).
- [31] S. R. White, D. J. Scalapino, R. L. Sugar, E. Y. Loh, J. E. Gubernatis and R. T. Scalettar, Phys. Rev. B, **40**, 506 (1989).
- [32] D.-H. Lee, Phys. Rev. Lett. **107**, 166806 (2011).
- [33] D. Friedan, Z. Qiu, and S. Shenker, Phys. Rev. Lett. **52**, 1575 (1984).
- [34] S. Chandrasekharan and U. J. Wiese, Phys. Rev. Lett. **83**, 16 (1999).
- [35] E. F. Huffman and S. Chandrasekharan, Phys. Rev. B **89**, 111101 (2014).
- [36] Z. C. Wei, C. Wu, Y. Li, S. Zhang, and T. Xiang, arXiv:1601.01994.

* yaohong@tsinghua.edu.cn

- [1] X.-G. Wen, *Quantum Field Theory of Many-body Systems*, (Oxford University Press, New York, 2004).
- [2] S. Sachdev, *Quantum Phase Transitions* (Cambridge University Press, Cambridge, ed. 2, 2011).
- [3] E. Fradkin, *Field Theories of Condensed Matter Physics, Second Edition*, (Cambridge University Press, Cambridge, 2013).

SUPPLEMENTARY MATERIALS

I. Proof of sign-problem-free for spinful and spinless interacting topological superconductor models

The topological superconductor of spin-1/2 electrons on the square lattice with attractive Hubbard interactions can be described by the following Hamiltonian:

$$H = \sum_{\langle ij \rangle, \sigma} [-tc_{i\sigma}^\dagger c_{j\sigma} + \Delta_{ij,\sigma} c_{i\sigma}^\dagger c_{j\sigma}^\dagger + h.c.] - \mu \sum_i (n_{i\uparrow} + n_{i\downarrow}) - U \sum_i n_{i\uparrow} n_{i\downarrow}, \quad (\text{S1})$$

where the triplet pairing amplitudes are given by $\Delta_{ij,\sigma} = \Delta$ for $j = i + \hat{x}$ and $\Delta_{ij,\sigma} = i\sigma\Delta$ for $j = i + \hat{y}$. We can express complex fermions by two components of Majorana fermions $c_j^\dagger = \frac{1}{2}(\gamma_j^1 + i\gamma_j^2)$ and $c_j = \frac{1}{2}(\gamma_j^1 - i\gamma_j^2)$, and then rewrite the Hamiltonian as:

$$H = H_0 + H_I, \\ H_0 = -\frac{t}{2} \sum_{\langle ij \rangle} \tilde{\gamma}_i^T \sigma^0 \tau^y \tilde{\gamma}_j + \frac{i\Delta}{2} \sum_{\langle ij \rangle_x} \tilde{\gamma}_i^T \sigma^0 \tau^x \tilde{\gamma}_j + \frac{i\Delta}{2} \sum_{\langle ij \rangle_y} \tilde{\gamma}_i^T \sigma^z \tau^z \tilde{\gamma}_j + \frac{\mu}{4} \sum_i \tilde{\gamma}_i^T \sigma^0 \tau^y \tilde{\gamma}_i, \quad (\text{S2})$$

$$H_I = -\frac{U}{4} \sum_i i\gamma_{i\uparrow}^1 \gamma_{i\uparrow}^2 i\gamma_{i\downarrow}^1 \gamma_{i\downarrow}^2, \quad (\text{S3})$$

where σ^α and τ^α are Pauli matrices acting in the spin and Majorana space respectively. We can perform HS transformation of attractive Hubbard term in density channel:

$$e^{\frac{U}{4} \Delta \tau i\gamma_{i\uparrow}^1 \gamma_{i\uparrow}^2 i\gamma_{i\downarrow}^1 \gamma_{i\downarrow}^2} = \sum_{\phi_i=\pm 1} e^{\lambda \phi_i (i\gamma_{i\uparrow}^1 \gamma_{i\uparrow}^2 + i\gamma_{i\downarrow}^1 \gamma_{i\downarrow}^2)}, \quad (\text{S4})$$

where ϕ_i represent auxiliary fields living on site i . Consequently, the decoupled Hamiltonian after Hubbard-Stratonovich (HS) transformation is:

$$\hat{h}(\phi) = \sum_{\langle ij \rangle, \sigma} -\frac{t}{2} \tilde{\gamma}_i^T \sigma^0 \tau^y \tilde{\gamma}_j + \sum_{\langle ij \rangle_x} \frac{i\Delta}{2} \tilde{\gamma}_i^T \sigma^0 \tau^x \tilde{\gamma}_j + \sum_{\langle ij \rangle_y} \frac{i\Delta}{2} \tilde{\gamma}_i^T \sigma^z \tau^z \tilde{\gamma}_j + \frac{\mu}{4} \sum_i \tilde{\gamma}_i^T \sigma^0 \tau^y \tilde{\gamma}_i + \lambda \sum_i \phi_i \tilde{\gamma}_i^T \sigma^0 \tau^y \tilde{\gamma}_i, \quad (\text{S5})$$

where $\tilde{\gamma}_i^T = (\gamma_{i\uparrow}^1, \gamma_{i\uparrow}^2, \gamma_{i\downarrow}^1, \gamma_{i\downarrow}^2)$. Because it respects these two anti-commuting MTR symmetries: $T_1^+ = \sigma^x \tau^z K$ and $T_2^- = i\sigma^y \tau^z K$, it belongs to the Majorana-class and is then sign-problem-free according to the theorem we have proved in the main text.

For the interacting topological superconductor of spinless fermions on the honeycomb lattice, the Hamiltonian at half-filling is given by

$$H = \sum_{\langle ij \rangle} (-tc_i^\dagger c_j + h.c.) + \sum_{\langle\langle ij \rangle\rangle} (\Delta c_i^\dagger c_j^\dagger + h.c.) + V \sum_{\langle ij \rangle} (n_i - 1/2)(n_j - 1/2). \quad (\text{S6})$$

Using the Majorana representation $c_j^\dagger = \frac{1}{2}[\gamma_j^1 + i\gamma_j^2(-1)^j]$ and $c_j = \frac{1}{2}[\gamma_j^1 - i\gamma_j^2(-1)^j]$, the Hamiltonian reads:

$$H = \sum_{\langle ij \rangle} -\frac{it}{2} \tilde{\gamma}_i^T \tau^z \tilde{\gamma}_j + \sum_{\langle\langle ij \rangle\rangle} i\Delta \tilde{\gamma}_i^T \tau^z \tilde{\gamma}_j - \frac{V}{4} \sum_{\langle ij \rangle} i\gamma_i^1 \gamma_i^2 i\gamma_j^1 \gamma_j^2, \quad (\text{S7})$$

where $\tilde{\gamma}_i^T = (\gamma_i^1, \gamma_i^2)$ and τ^α are Pauli matrices acting in the Majorana space. We perform HS transformation of nearest-neighbor interaction in hopping channel:

$$e^{\frac{V}{4} \Delta \tau i\gamma_i^1 \gamma_i^2 i\gamma_j^1 \gamma_j^2} = \sum_{\phi_{ij}=\pm 1} e^{\lambda \phi_{ij} (i\gamma_i^1 \gamma_j^1 - i\gamma_i^2 \gamma_j^2)}, \quad (\text{S8})$$

where ϕ_{ij} are auxiliary fields living on NN bonds. We then obtain the decoupled Hamiltonian after HS transformation

$$\hat{h}(\phi) = \sum_{\langle ij \rangle} -\frac{it}{2} \tilde{\gamma}_i^T \tau^z \tilde{\gamma}_j + \sum_{\langle\langle ij \rangle\rangle} i\Delta \tilde{\gamma}_i^T \tau^z \tilde{\gamma}_j + i\lambda \sum_{\langle ij \rangle} \phi_{ij} \tilde{\gamma}_i^T \tau^z \tilde{\gamma}_j, \quad (\text{S9})$$

which is invariant under the following two anti-commuting MTR symmetries: $T_1^+ = \tau^x K$ and $T_2^- = i\tau^y K$, and then belongs to the Majorana-class which is sign-problem-free.

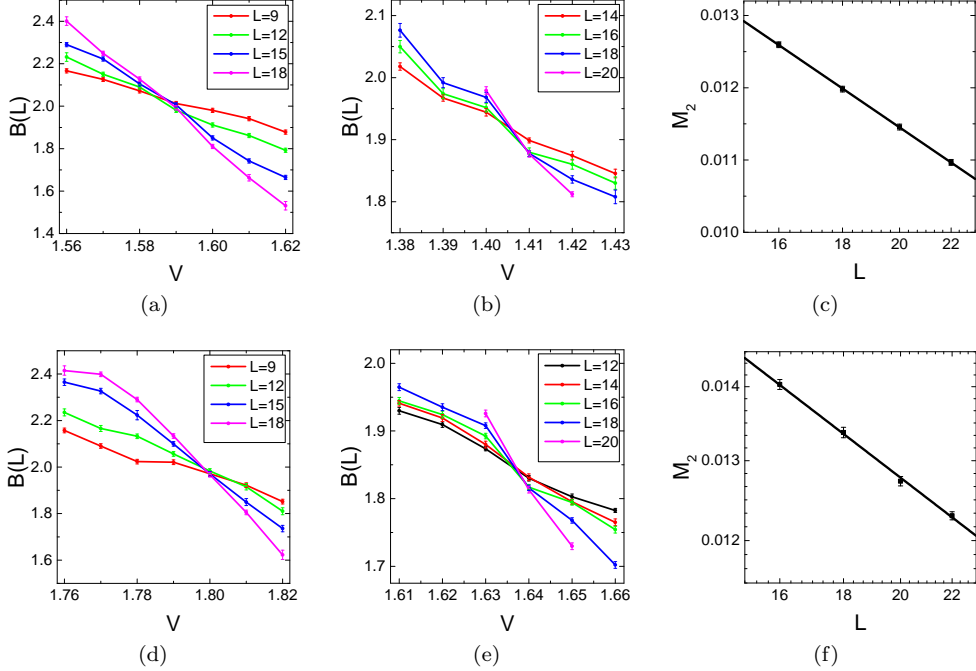


FIG. S1. Emergent SUSY at the edge QCP in the topological superconductor of spinless fermions on the honeycomb lattice studied by the sign-problem-free Majorana QMC. (a-c) QMC results for $\Delta = 0.1t$. From the Binder ratio on the edge and on the bulk, the edge and bulk QCPs occur at $V_c^{\text{edge}} \approx 1.41$ and $V_c^{\text{bulk}} \approx 1.59$, respectively. From the log-log plot of the structure factor $M_2(L)$ versus L at the edge QCP $V = V_c^{\text{edge}}$, the anomalous dimension η fitted from the slope is $\eta = 0.41 \pm 0.01$, which is almost perfectly consistent with exact value of 0.40 predicted by the emergent SUSY. (d-e) QMC results for $\Delta = 0.2$. From the Binder ratio on the edge and on the bulk, the edge and bulk QCPs occur at $V_c^{\text{edge}} \approx 1.64$ and $V_c^{\text{bulk}} \approx 1.80$, respectively. From the log-log plot of the structure factor $M_2(L)$ versus L at the edge QCP $V = V_c^{\text{edge}}$, the anomalous dimension η fitted from the slope is $\eta = 0.42 \pm 0.02$, which is nearly perfectly consistent with the exact value predicted by the emergent SUSY.

II. Details of the projector MQMC simulation and the Binder ratio

We use projector QMC in Majorana representation to study interacting topological superconductor. In projector QMC, the expectation value of the observable in ground state can be evaluated as:

$$\frac{\langle \psi_0 | O | \psi_0 \rangle}{\langle \psi_0 | \psi_0 \rangle} = \lim_{\theta \rightarrow \infty} \frac{\langle \psi_T | e^{-\theta H} O e^{-\theta H} | \psi_T \rangle}{\langle \psi_T | e^{-2\theta H} | \psi_T \rangle}, \quad (\text{S10})$$

where ψ_0 is the true ground state wave function and ψ_T is a trial wave function which should have a finite overlap with ground state wave function. In our computation of the systems with periodic boundary condition, the imaginary-time projection parameter is $\theta = 60/t$. In the cases of open boundary condition, most systems are computed using $\theta = 90/t$ and some systems with large systems size or near critical points are computed using $\theta = 120/t$. We have checked that results stay nearly the same for larger θ . We set $\Delta\tau = 0.05$. The results do not change if we use smaller $\Delta\tau$. Because of absence of sign-problem, we can perform large-scale QMC simulations. In the computation of bulk phase transition, we use periodic boundary condition. The largest systems size is $N = 2 \times 18 \times 18$ for the spinless interacting topological superconductor on honeycomb lattice and $N = 20 \times 20$ for the spinful interacting topological superconductor on square lattice. In the computation of edge phase transition, we use periodic boundary condition in x direction and open boundary condition in y direction. The largest systems size is $N = 2 \times 22 \times 11$ for the case of spinless fermions and $N = 22 \times 22$ for the case of spin-1/2 electrons.

As a powerful numerical technique, Binder ratio $B(L) = \frac{M^4}{(M^2)^2}$ is frequently used to determine quantum critical points. For CDW phase transition, M_2 is the CDW structure factor: $M_2 = \sum_{ij} \frac{\eta_i \eta_j}{N^2} \langle (n_i - \frac{1}{2})(n_j - \frac{1}{2}) \rangle$ and $M_4 = \sum_{ijkl} \frac{\eta_i \eta_j \eta_k \eta_l}{N^4} \langle (n_i - \frac{1}{2})(n_j - \frac{1}{2})(n_k - \frac{1}{2})(n_l - \frac{1}{2}) \rangle$, where $\eta_i = +1(-1)$ on $A(B)$ sublattice. For singlet superconductivity phase transition, M_2 is the s-wave singlet-pairing structure factor: $M_2 = \sum_{ij} \frac{1}{N^2} \langle (c_{i\uparrow}^\dagger c_{i\downarrow}^\dagger - c_{i\downarrow} c_{i\uparrow})(c_{j\uparrow}^\dagger c_{j\downarrow}^\dagger - c_{j\downarrow} c_{j\uparrow}) \rangle$ and $M_4 = \sum_{ijkl} \frac{1}{N^4} \langle (c_{i\uparrow}^\dagger c_{i\downarrow}^\dagger - c_{i\downarrow} c_{i\uparrow})(c_{j\uparrow}^\dagger c_{j\downarrow}^\dagger - c_{j\downarrow} c_{j\uparrow})(c_{k\uparrow}^\dagger c_{k\downarrow}^\dagger - c_{k\downarrow} c_{k\uparrow})(c_{l\uparrow}^\dagger c_{l\downarrow}^\dagger - c_{l\downarrow} c_{l\uparrow}) \rangle$. In the computation of phase

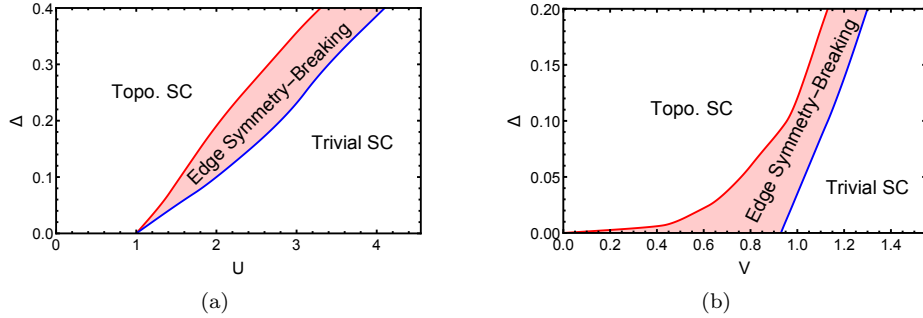


FIG. S2. The quantum phase diagram from mean-field calculations. (a) The spinful topological superconductor on the square lattice. In red region, the edge states are gapped out by having a finite singlet pairing component which spontaneously break the Z_2 symmetry while bulk is disordered and topologically nontrivial; (b) The spinless topological superconductor on the honeycomb lattice. In red region, the edge states is gapped out by spontaneously breaking the particle-hole symmetry while the bulk is still topologically nontrivial.

transition at bulk, we simulate M_2 and M_4 by a summation over all the sites. While in the computation of phase transition at edge, we only sum over the sites at the boundary ($y = 0$ and $y = L_y$). In disordered phase, Binder ratio increases as the systems size in increased, while in ordered phase its trend is opposite. The Binder ratio for different L should cross at the critical point.

V. QMC results of interacting topological superconductors and emergent SUSY

For the interacting topological superconductor of spin-1/2 electrons on the square lattice, we use Binder ratio to determine the quantum phase transitions in the bulk and on the edge, respectively. We set $\Delta = 0.3$ and $\mu = -0.5$ in our QMC simulations. From the Binder ratio on the edge, the edge QCP occurs $U_c^{\text{edge}} = 4.04$ while from the Binder ratio in the bulk, the bulk QCP happens at a stronger interaction strength $U_c^{\text{bulk}} = 4.575$. Moreover, from the log-log plot of the structure factor $M_2(L)$ versus L at the edge QCP $U = U_c^{\text{edge}}$, the anomalous dimension η fitted from the slope is $\eta = 0.43 \pm 0.04$, which is almost perfectly consistent with exact value of 0.40 predicted by the emergent SUSY.

For the interacting topological superconductor of spinless fermions on the honeycomb lattice described by Eq. (S6), it is a p -wave topological superconductor hosting helical edge states which are protected by the particle-hole symmetry $P = T_1^+ T_2^- = \tau^z$. At large V , we expect a quantum phase transition to the topologically-trivial phase which spontaneously breaks the particle-hole symmetry P . Remarkably, the spontaneous symmetry breaking on the edge and in the bulk happen at different values of V and the edge quantum phase transition occurs first. For $\Delta = 0.1t$, from the Binder ratio on the edge and on the bulk, the edge and bulk QCPs occur at $V_c^{\text{edge}} = 1.41$ and $V_c^{\text{bulk}} = 1.59$, respectively. From the log-log plot of the structure factor $M_2(L)$ versus L at the edge QCP $V = V_c^{\text{edge}}$, the anomalous dimension η fitted from the slope is $\eta = 0.41 \pm 0.01$, which is almost perfectly consistent with exact value of 0.40 predicted by the emergent SUSY. For $\Delta = 0.2t$, from the Binder ratio on the edge and on the bulk, the edge and bulk QCPs occur at $V_c^{\text{edge}} = 1.64$ and $V_c^{\text{bulk}} = 1.80$, respectively. From the log-log plot of the structure factor $M_2(L)$ versus L at the edge QCP $V = V_c^{\text{edge}}$, the anomalous dimension η fitted from the slope is $\eta = 0.42 \pm 0.02$, which is also consistent with exact value of 0.40 predicted by the emergent SUSY.

IV. The mean-field studies of the topological superconductors with interactions

We also performed self-consistent mean-field calculations to study the quantum phase diagrams of the two topological superconductor models mentioned in main text. For the spinful topological superconductors on the square lattice, we study the mean-field QCPs on the boundary and in the bulk, respectively, and the mean-field quantum phase diagram is shown in Fig. S2(a). For the spinless superconductor on honeycomb lattice, we study the mean-field quantum critical points of the zigzag boundary and bulk, respectively. In Fig. S2(b), we show that when Δ is close to zero, the edge critical V approaches to zero. This is because of the flat dispersion of the zigzag edge state when $\Delta = 0$. For any finite Δ , the edge critical value is always smaller than the bulk one such that there is a finite region with only edge symmetry-breaking.